Increased Synaptic Strength and mGlu$_{2/3}$ Receptor Plasticity on Mouse Prefrontal Cortex Intra-telencephalic Pyramidal Cells Following Intermittent Access to Ethanol

Max E. Joffe[†,a,b,c], **Danny G. Winder**[a,c,d], **P. Jeffrey Conn**[a,b,c]

[a.]Department of Pharmacology, Vanderbilt University, Nashville, TN, 37232, USA.

[b.]Warren Center for Neuroscience Drug Discovery, Nashville, TN, 37232, USA

[c.]Vanderbilt Center for Addiction Research, Nashville, TN, 37232, USA

[d.]Department of Molecular Physiology and Biophysics, Vanderbilt University, Nashville, TN, 37232, USA

Abstract

Background.—The medial prefrontal cortex (PFC) is crucial for regulating cravings and alcohol-seeking in alcohol use disorder (AUD) patients and animal models. Maladaptive changes in volitional ethanol intake have been associated with PFC function, yet synaptic adaptations within PFC have not been consistently detected in voluntary drinking rodent models. At least 80% of the neurons in PFC are glutamatergic pyramidal cells. Pyramidal cells provide the predominant cortical output to several brain regions relevant to alcohol use disorder, including structures within the telencephalon (IT; e.g. basal ganglia, amygdala, other neocortical regions,) and also outside the telencephalon (ET; e.g. lateral hypothalamus, midbrain monoaminergic structures, thalamus).

Methods.—In addition to their anatomical distinctions, studies from several laboratories have revealed that prefrontal cortical IT and ET pyramidal cells may be separated by specific electrophysiological parameters. These distinguishable parameters provide opportunities to readily classify pyramidal cells into separable subtypes. Here, we employed and validated the hyperpolarization sag ratio as a diagnostic proxy for separating ET (Type A) and IT (Type B) neurons. We recorded from deep layer prelimbic PFC pyramidal cells of mice one day after 4–5 weeks of intermittent access (IA) ethanol exposure.

Results.—Membrane properties were not altered by IA ethanol, but excitatory postsynaptic strength onto IT Type B neurons was selectively enhanced in slices from IA ethanol mice. The increased excitatory drive was accompanied by enhanced mGlu$_{2/3}$ receptor plasticity on IT Type B

neurons, providing a potential translational approach to mitigate cognitive and motivational changes to PFC function related to binge drinking.

Conclusions.—Together, these studies provide insight into the specific PFC neurocircuits altered by voluntary drinking. In addition, these findings provide additional rationale for developing compounds that potentiate $mGlu_2$ and/or $mGlu_3$ receptor function as potential treatments for AUD.

Keywords

binge drinking; prefrontal cortex; mGlu receptor; synaptic physiology; synaptic plasticity

1. Introduction

Functional alterations within the medial prefrontal cortex (PFC) are critically linked with the ability to regulate cravings and alcohol-seeking in alcohol use disorder (AUD) patients and animal models (Abernathy et al., 2010; Blaine et al., 2020; Koob and Volkow, 2016). Mechanistic studies to examine PFC dysfunction in rodent models have most often used chronic intermittent ethanol (CIE) vapor exposure to achieve high levels of ethanol exposure and dependence. Following CIE and other models of chronic ethanol administration, several groups have demonstrated, in general, that reduced inhibition and enhanced excitatory synaptic activity characterize dependence-related changes in PFC physiology (Bohnsack et al., 2018; Centanni et al., 2017; Hughes et al., 2019; Kroener et al., 2012; Pava and Woodward, 2014; Pleil et al., 2015; Varodayan et al., 2018). On the other hand, despite the compelling data linking maladaptive changes in volitional drinking with PFC dysfunction (Haun et al., 2018; Radke et al., 2017; Salling et al., 2018; Seif et al., 2013; Siciliano et al., 2019), synaptic adaptations to PFC pyramidal cells have been limited following voluntary ethanol intake (Cannady et al., 2020; Crowley et al., 2019; Klenowski et al., 2016). This disconnect between behavior and physiology raises the possibility that subtypes of PFC pyramidal cells exhibit distinct adaptations following volitional ethanol intake.

Pyramidal cells comprise at least 80% of the neurons in PFC and provide the predominant output from the structure (Abernathy et al., 2010). Pyramidal cells arising from the deep layers of the PFC course onto many targets that regulate cognitive and motivated behaviors related to and including drinking (Gabbott et al., 2005). These downstream structures include basal ganglia nuclei, monoaminergic midbrain nuclei, sites within the extended amygdala, and the lateral hypothalamus. Dense, reciprocal connectivity with thalamic nuclei has also been described as a defining feature of PFC anatomy (Carlen, 2017; Uylings et al., 2003). Studies from several laboratories have revealed that PFC pyramidal cells can be generally segregated into two types based on morphology, anatomical connections, and specific electrophysiological parameters. In general, Type A neurons display extensive dendritic arborizations into superficial cortical layers and generally project to subcortical structures (Anastasiades et al., 2018b; Collins et al., 2018; Gee et al., 2012; Morishima et al., 2011). As such, they have been described as extra-telencephalic (ET) neurons and this group also includes pyramidal tract neurons. Intra-telencephalic (IT) neurons, by contrast, project to contralateral cortex as well as other sites within the forebrain, including the striatum, amygdala, septum, and other cortical regions. IT neurons generally display narrow or limited

dendritic arborizations and have been described as Type B neurons. In addition to these anatomical and structural differences, several membrane physiology parameters of ET Type A and IT Type B pyramidal cells diverge in a distinguishing manner (Anastasiades et al., 2018a; Anastasiades et al., 2018b; Collins et al., 2018; Dembrow et al., 2010; Gee et al., 2012; Lee et al., 2014; Leyrer-Jackson and Thomas, 2019). Owing primarily to high expression of hyperpolarization-activated cation (HCN) channels (Salling et al., 2018; Shah, 2014), the membrane potential of Type A neurons undergoes a rebound depolarization following negative current injections, often described as a "hyperpolarization sag". Type B neurons, instead, generally lack this pronounced sag current. Open HCN channels also modulate the membrane resistance (R_m) of PFC pyramidal cells, such that Type A neurons have more channels and an accordingly lower R_m, while Type B neurons display higher R_m. These readily distinguishable membrane physiology parameters provide opportunities to leverage functional differences to classify pyramidal cell into separable subtypes. In this manner, the hyperpolarization sag may be used as a diagnostic proxy for separating ET Type A and IT Type B neurons.

Importantly, previous studies have shown modest or no changes when measuring excitatory synaptic strength onto pyramidal cells following voluntary drinking (Cannady et al., 2020; Crowley et al., 2019; Klenowski et al., 2016). In addition, some of the previous findings apparently conflict with each other, providing motivation to investigate mechanisms through which ethanol alters PFC synaptic transmission. The heterogeneous nature of deep layer pyramidal cells suggests that subtle changes to a discrete subset might be obfuscated in experiments that have not classified them into smaller groups. Thus, we reasoned that stratifying pyramidal cells might uncover cell type-specific synaptic adaptations following voluntary drinking. To test this hypothesis, we recorded from deep layer pyramidal cells of mice one day after 4–5 weeks of intermittent access (IA) ethanol exposure, initiated in young adulthood. IA ethanol did not alter intrinsic physiological parameters in the adult PFC, and we proceeded to classify pyramidal cells as Type A or Type B based on the hyperpolarization sag ratio. In striking contrast, we observed cell type-specific adaptations to synaptic physiology, whereby excitatory synaptic strength onto IT Type B neurons was selectively enhanced in slices from IA ethanol mice. The increased excitatory drive was accompanied by enhanced mGlu$_{2/3}$ receptor plasticity on IT Type B neurons, providing a potential translational approach to mitigate cognitive and motivational changes to PFC function related to binge drinking.

2. Material and Methods

2.1. Mice

Mice were housed on a standard 12-hour light cycle (on at 6:00 am). For retrograde labelling experiments, female and male C57BL6/J mice were purchased from Jackson Laboratories and recordings were made from tdTomato-expressing pyramidal cells. For IA ethanol experiments, mice were bred in-house on a congenic C57BL6/J background to express tdTomato in PFC interneurons. Female PV-Cre mice (Jackson Laboratories, Stock No: 017320) or SST-Cre mice (Jackson Laboratories, Stock No: 028864) were crossed with male Rosa26-loxP-STOP-loxP-CAG-tdTomato "Ai9" mice (Jackson Laboratories, Stock No:

007909). Recordings from interneurons were made for a previous set of studies (Joffe et al., 2020b). For IA ethanol experiments described in this manuscript, recordings were made from non-fluorescent neurons that displayed pyramidal cell characteristics, including large capacitance and spike-firing adaption. All mice were used for experiments. Mice were crudely classified as female or male based on external genitalia. Trends for each key physiological finding emerged in neurons from both female mice and male mice (Figure S2), therefore all data were pooled for the primary analyses. Mice were group-housed from weaning until 6 weeks of age, after which they were individually housed for IA ethanol exposure in clear polysulfone individually ventilated cages (NexGen Mouse 900, Allentown Incorporated).

2.2   Intermittent access (IA) to ethanol

IA ethanol engenders higher levels of ethanol exposure than continuous access (Hwa et al., 2011), and C57BL/6J mice drink more ethanol than other strains (Belknap et al., 1993; Boyce-Rustay et al., 2008; Rodgers and Mc, 1962). We initiated IA ethanol during young adulthood (6–7 weeks). With constant access to food and water, mice were provided ethanol in their home cages for alternating 24-hour periods. Ethanol was prepared in reverse-osmosis water from 95% undenatured ethyl alcohol (Decon Labs, Incorporated). Falcon tubes (50-mL) capped with rubber stoppers (Fisherbrand 14–135H, Fisher Scientific) and open tip straight tubes (OT100, Ancare) were used to deliver ethanol and water. Tube weight was measured before and after each session and the average drip (0.2 g) was subtracted from all values. Ethanol was provided and removed 3–4 hours prior to the transition to the dark cycle. The ethanol concentration was slowly ramped up to 20% ethanol during the first week, after which 20% ethanol as provided for the remainder of the study. Female mice drank relatively more ethanol than male littermates (30.2 ± 2.5 vs 22.6 ± 1.7 g/kg/day, $p < 0.05$, Mann-Whitney U test); all drinking data was presented in a previous publication (Joffe et al., 2020b). Previous studies have demonstrated that C57BL6/J mice typically achieve intoxicating blood ethanol concentrations (~80 mg/dL) under these conditions (Hwa et al., 2011; Salling et al., 2018).

2.3   Electrophysiology

After 3–4 weeks of 20% ethanol intake, we assessed pyramidal cell intrinsic and synaptic physiological parameters using patch-clamp electrophysiology. One day (16–20 hours) following the last period of ethanol availability, mice were sacrificed and acute prelimbic PFC slices were made as described (Di Menna et al., 2018; Joffe et al., 2020b). Mice were decapitated under deep isoflurane anesthesia. Brains were rapidly removed, and coronal slices (300 μM) were prepared (22–24 °C) and recovered (30–32 °C, 10 minutes) in *N*-methyl-D-glucamine solution. Slices recovered for at least an additional hour (22–24 °C) in artificial cerebrospinal fluid, containing (in mM): 119 NaCl, 2.5 KCl, 2.5 $CaCl_2$, 1.3 $MgCl_2$, 1 NaH_2PO_4, 11 glucose, and 26 $NaHCO_3$. Cells were patched with a potassium-based internal solution (in mM): 125 K-gluconate, 4 NaCl, 10 HEPES, 4 MgATP, 0.3 NaGTP, 10 Tris-phosphocreatine. Following 5-minutes dialysis, membrane physiological parameters were evaluated in current-clamp configuration. A series of 20, 1-sec current injections were delivered from −150 pA to +300 pA, incremented by 25 pA. Membrane resistance (R_m) was determined by the best-fit slope or the membrane potential hyperpolarization relative to the

injected current. Sag ratio was evaluated based on the resting membrane potential (V_m) and hyperpolarization in response to negative current injections. Sag ratio was calculated as the difference between the peak and steady-state hyperpolarizations, normalized to the steady-state to account for cell-to-cell variation in R_m (Joffe et al., 2020a). The sag ratio for each cell was taken as the average value across the 3 most-negative current injections per cell. The medium afterhyperpolarization (mAHP) was calculated as the amplitude of the membrane potential decrease during the 0.5-sec period after a current injection resulted in >10 action potentials (generally 100–200 pA for pyramidal cells). Cells were then switched to voltage-clamp configuration for 3–4 minutes, and spontaneous excitatory synaptic transmission was evaluated during the last 2-minute period. Cells were clamped near the chloride reversal potential, at −80 mV, to electrically isolate excitatory postsynaptic currents (EPSCs) as empirically confirmed (Joffe et al., 2020b). Spontaneous excitatory postsynaptic currents (sEPSCs) were detected with a pre-defined template for pyramidal cells. Finally, in some cells, long-term recordings of evoked EPSCs were made using paired pulses of local electrical stimulation (5–50 μA, 0.1 ms, 50 ms ISI) of superficial layer 5 at 0.1 Hz. The mGlu$_{2/3}$ agonist LY379268 (200 nM, 10 minutes) was applied to elicit LTD (Di Menna et al., 2018; Joffe et al., 2017; Joffe et al., 2020a; Joffe et al., 2019). We routinely collected 2–3 cells per slice, and slices were discarded following any experiment involving drug application. Slice treatment and data collection protocols were identical in all groups.

2.4 Stereotaxic injections

For some studies, stereotaxic viral injections were performed as described (Joffe et al., 2020a). Briefly, mice were anesthetized with isoflurane and 200–300 nL retrograde adeno-associated virus (AAVrg-CAG-tdTomato, titer 7×10^{12} vg/mL; Addgene viral prep #59462-AAVrg; gift from Edward Boyden) was delivered unilaterally to a PFC efferent structure. ET target sites included the lateral hypothalamus (LH; −1.2 ML, −1.6 AP, −5.6 DV) and ventral tegmental area (VTA; −0.5 ML, −3.0 AP, −5.4 DV). IT target sites included the basolateral amygdala (BLA; −3.2 ML, −1.6 AP, −5.0 DV), dorsomedial striatum (DMS; −1.2 ML, 1.2 AP, −3.4 DV), and nucleus accumbens (NAC; −0.8 ML, 1.2 AP, −4.6 DV). Recordings were only made from animals where faithful and restricted expression was observed at the injection site, as confirmed by tdTomato fluorescence immediately after slice preparation. DMS and NAC injection sites were confirmed in 300 um slices near the PFC. LH, VTA, and BLA injection sites were confirmed in thick (~1 mm) slices. The characteristic distributions of pyramidal cell somas across cortical layers and subregions was consistent with prior studies (Gabbott et al., 2005). Recordings from DMS- and NAC-projecting pyramidal cells were performed on the contralateral hemisphere relative to the injection site, while all other recordings were made from ipsilateral pyramidal cells.

2.5 Statistics

The number of cells or mice per group is respectively denoted by "n" and/or "N" in each figure legend. Data are generally presented as cumulative distributions, mean ± standard error, or as box plots displaying median, interquartile range, and range. Analyses were performed in GraphPad Prism. Two-way ANOVA and the Mantel-Cox test were used as appropriate. Where we observed a significant (α: 0.05) main effect of cell type or a significant interaction between cell type and IA ethanol, we followed up with Sidak post-hoc

comparisons. For current-evoked spiking, a three-way ANOVA did not reveal any significant main effect or interaction related to IA ethanol and no further analyses were performed. All statistical findings are displayed in the figures or figure legends.

3.   Results

Virus-assisted circuit mapping confirms ET and IT pyramidal cells respectively display Type A and Type B electrophysiological signatures.

Several laboratories have demonstrated that ET and IT pyramidal cells display quantitative differences in hyperpolarization sag and other physiological properties (Anastasiades et al., 2018a; Anastasiades et al., 2018b; Gee et al., 2012; Lee et al., 2014; Seong and Carter, 2012). To confirm this finding, we expressed the fluorescent reporter tdTomato in discrete populations of pyramidal cells by delivering a retrograde AAV to AUD-relevant brain regions that receive monosynaptic projections from PFC (Gabbott et al., 2005). The non-exhaustive set of five efferent structures was distributed across the midbrain [ET; lateral hypothalamus (LH) and ventral tegmental area (VTA)] and forebrain [IT; basolateral amygdala (BLA), dorsomedial striatum (DMS), and nucleus accumbens (NAC)] (Figure 5A), thus providing an opportunity to map specific physiological parameters onto pyramidal cell projection type. All recordings were made in superficial layer 5 of the prelimbic cortex (sometimes referred to as 5a). We found that fluorescent labeling following retrograde viral targeting of the NAC, DMS, LH, and VTA, was most intense throughout this layer (consistent with patterns observed by (Gabbott et al., 2005). Pyramidal cells that target the BLA were more abundant in layers 2/3, but a substantial number of labeled cells were also present in layer 5. Consistent with previous studies, ET and IT cells displayed considerable heterogeneity with respect to membrane physiology and clearly separated into two clusters based on R_m and the hyperpolarization sag ratio (Figure 1). Indeed, we observed major differences in sag ratio (Figure 2A, One-way ANOVA $F_{4,48} = 30.3$, $p < 0.0001$) and R_m (Figure 2B, One-way ANOVA $F_{4,49} = 15.7$, $p < 0.0001$) across pyramidal cell type. LH- and VTA-projecting neurons displayed substantial hyperpolarization sag and low R_m, whereas IT neurons displayed relatively minimal rebound sag and high resistance. Not all intrinsic parameters exhibited clear IT/ET differences, however, as no relationship between V_m and pyramidal cell type was detected (Figure 2C, One-way ANOVA $F_{4,49} = 1.11$, n.s.). Furthermore, while the magnitude of mAHP varied in relation to pyramidal cell target, we did not observe clear separation between ET and IT neurons (Figure 2D, One-way ANOVA $F_{4,50} = 3.23$, $p < 0.02$). Finally, we examined basal synaptic strength and demonstrated differences in sEPSC amplitude (Figure 2E, One-way ANOVA $F_{4,48} = 7.30$, $p < 0.001$) and frequency (Figure 2F, One-way ANOVA $F_{4,49} = 3.56$, $p < 0.02$) across pyramidal cell types. As expected from previous studies (Anastasiades et al., 2018b; Joffe et al., 2020a; Morishima et al., 2011), ET neurons exhibit greater synaptic inputs, on average, than IT cells. Taken together, this limited survey confirms that several independent intrinsic and synaptic properties vary based on pyramidal cell projection target.

We sought to use this dataset to develop a simple quantitative means to separate ET and IT cells in circumstances where fluorescent labeling is not tractable. The sag ratio appeared particularly useful for this aim. Our dataset included 30 ET cells and 23 IT cells (56.6% ET

vs 43.4%IT); therefore, we calculated the sag ratio corresponding to the 56.6 percentile of this dataset. We reasoned this value (0.12) could be used as a standalone criterion to segregate unlabeled layer 5 pyramidal cells sampled at random.

Pyramidal cells from adult mice provided IA ethanol exhibit comparable hyperpolarization sag relative to controls.

We previously reported on adaptations to fluorescently labeled PFC interneurons following IA ethanol (Joffe et al., 2020b). Mice were sacrificed for electrophysiology one day following the final period of ethanol availability (Figure 3A). In addition to the recordings from inhibitory interneurons, we recorded from unlabeled pyramidal cells in the same slices and aimed to use the hyperpolarization sag ratio as a means to discriminate between ET Type A and IT Type B pyramidal cells (Anastasiades et al., 2018b; Clarkson et al., 2017; Dembrow et al., 2010; Gee et al., 2012; Lee et al., 2014; Morishima et al., 2011; Seong and Carter, 2012). To employ this approach, we first needed to ascertain that hyperpolarization sag is not affected by IA ethanol exposure to adult mice, as such an effect could confound later interpretations. Indeed, pyramidal cells from IA ethanol mice and matched controls displayed no differences in the hyperpolarization sag frequency distribution (Figure 3B, χ^2 = 1.52, df = 1, n.s., Log-rank Mantel-Cox test). Pyramidal cells appeared roughly split into two groups with sag ratios less than and greater than our criterion of 0.12. Because this frequency distribution was not affected by IA ethanol, we reasoned that the sag ratio is an appropriate diagnostic tool to functionally demarcate pyramidal cells.

Stratifying pyramidal cells by sag ratio yields two cell types with separable physiological parameters

Based on our findings, we split pyramidal cells based on the sag ratio magnitude relative to 0.12. Cells with large sag ratios were classified as Type A putative ET pyramidal cells, whereas those with relatively low sag ratios were considered Type B IT pyramidal cells (Figure 3C). We further confirmed that IA ethanol does not affect the sag ratio in either cell type (Figure 4B, Two-way ANOVA IA ethanol: $F_{1,52} = 0.700$, n.s.; cell type × IA ethanol interaction: $F_{1,52} = 0.266$, n.s.), and then assessed several parameters with known differences across pyramidal cell type. Consistent with previous studies, Type B cells displayed high R_m (Figure 4C, Two-way ANOVA cell type: $F_{1,47} = 32.1$, p < 0.0001; IA ethanol: $F_{1,47} = 3.52$, p < 0.07; cell type × IA ethanol interaction: $F_{1,47} = 3.41$, p < 0.08) and small mAHP (Figure 4D, Two-way ANOVA cell type: $F_{1,47} = 19.7$, p < 0.0001; IA ethanol: $F_{1,47} = 1.03$, n.s.; cell type × IA ethanol interaction: $F_{1,47} < 0.001$, n.s.) relative to nearby Type A neurons. No effect of IA ethanol was observed regarding either R_m or mAHP, and neither cell type nor IA ethanol affected V_m (Figure 4E, Two-way ANOVA cell type: $F_{1,47} = 0.83$, n.s.; IA ethanol: $F_{1,47} = 0.56$, n.s.; cell type × IA ethanol interaction: $F_{1,47} = 0.05$, n.s.). Finally, consistent with previous work, Type B cells exhibited greater current-evoked spiking relative to Type A neurons (Figure 4F and S1, Three-way repeated-measures ANOVA, cell type: $F_{1,46} = 15.7$, p < 0.003; cell type × current interaction: $F_{12,552} = 11.3$, p < 0.0001). Other than this expected difference between cell types, no main effect or interaction with IA ethanol affected spike-firing properties. Taken together, these data confirm that the hyperpolarization sag ratio may be used as a simple and effective criterion to split PFC pyramidal cells into two classes. IA

ethanol exposure to adult mice, at this single one-day abstinence timepoint, had no effect on several membrane physiology parameters overall or in either pyramidal cell type.

IA ethanol selectively potentiates excitatory synaptic strength onto Type B pyramidal cells

We next examined excitatory drive onto pyramidal cells by electrically isolating glutamatergic sEPSCs in voltage-clamp configuration. In general, changes in sEPSC amplitude are consistent with adaptations to quantal size, or the function of postsynaptic AMPA receptors, whereas the frequency of sEPSCs is regulated by quantal content, i.e. a combination of presynaptic release probability and the number of sampled synapses. Consistent with prior accounts (Anastasiades et al., 2018b; Joffe et al., 2020a; Morishima et al., 2011), Type B neurons displayed smaller sEPSC amplitudes than Type A cells overall (Figure 5A and 5B, Two-way ANOVA cell type: $F_{1,46} = 19.6$, $p < 0.0001$; IA ethanol: $F_{1,46} = 4.34$, $p < 0.05$). More interesting, IA ethanol treatment was associated with increased sEPSC amplitude overall, and post hoc tests confirmed a selective increase in Type B cells ($p < 0.05$ Sidak post-test). Adaptations related to IA ethanol were restricted to sEPSC amplitude. On average, Type B cells exhibited lower sEPSC frequency, but IA ethanol did not affect this parameter (Figure 5C, Two-way ANOVA cell type: $F_{1,47} = 5.44$, $p < 0.03$; IA ethanol: $F_{1,47} = 0.004$, n.s.). Similarly, the PPR of electrically-evoked EPSCs was lower on Type B relative to Type A cells and no effect of IA ethanol was observed (Figure 5D, Two-way ANOVA cell type: $F_{1,24} = 8.55$, $p < 0.01$; IA ethanol: $F_{1,24} = 0.169$, n.s.). In sum, these findings collectively suggest that IA ethanol treatment increases postsynaptic strength onto a distinct subtype of PFC pyramidal cells. Based on this, we reasoned that synaptic plasticity mechanisms that regulate synaptic strength might also be affected in Type B cells following IA ethanol.

IA ethanol enhances LTD in Type B cells driven by mGlu$_{2/3}$ receptors.

We have recently described forms of LTD regulated by mGlu$_2$ and mGlu$_3$ receptors in PFC (Di Menna et al., 2018; Joffe et al., 2017; Joffe et al., 2020a; Joffe et al., 2019). mGlu$_3$ receptors can initiate a postsynaptic signaling cascade that culminates with AMPA receptor internalization. By contrast, mGlu$_2$ receptors can facilitate a presynaptically expressed form of LTD that occurs at inputs from the mediodorsal thalamus (MDT), but not at other afferents (Figure 6A). To elicit LTD, we applied the orthosteric mGlu$_{2/3}$ agonist LY379268 (LY379, 200 nM, 10 minutes) while performing long-term recordings from classified pyramidal cells. LY379268 induced LTD of excitatory transmission onto Type A neurons in a similar manner in cells from control and IA ethanol mice (Figure 6B, 6D, and 6E). Based on the increased synaptic strength onto IA ethanol Type B neurons, we expected to observe a facilitation of mGlu receptor-driven LTD in those cells. Indeed, Type B cells from IA ethanol mice exhibited greater LTD than control Type B cells (Figure 6C, 6D, and 6E, Two-way ANOVA cell type × IA ethanol interaction: $F_{1,23} = 9.27$, $p < 0.006$; $p < 0.05$ Sidak post-test). In general, the LTD evoked by LY379268 at electrically-evoked EPSCs is predominantly mediated by postsynaptic mGlu$_3$ signaling and does not affect PPR or other measurements of presynaptic glutamate release (Joffe et al., 2017). However, we were struck by a pronounced increase in PPR associated with LTD in Type B cells from IA ethanol mice (Figures 6F and 6G, Two-way ANOVA cell type × IA ethanol interaction: $F_{1,22} = 6.83$, $p < 0.02$; $p < 0.05$ Sidak post-test), suggesting that IA ethanol may enhance or unmask a

predominant presynaptic form of LTD. Similar findings were obtained in female mice and in male mice (Figure S2). Taken together, these data confirm that IA ethanol exerts differential effects on the function of excitatory synapses across pyramidal cell subtypes, and further implicate differences in the ability of mGlu$_{2/3}$ receptors to modulate PFC subcircuit elements.

4. Discussion

Binge drinking affects PFC circuit function, yet robust synaptic adaptations to pyramidal cells have not been consistently observed in rodent models. To address this gap, we segregated deep layer prelimbic pyramidal cells into ET Type A and IT Type B neurons based on their intrinsic physiology. Viral-assisted circuit mapping confirmed that the hyperpolarization sag ratio, by itself, can effectively classify pyramidal cells as ET or IT. Using this approach, we uncovered cell type-specific adaptations following IA ethanol, whereby binge drinking enhanced postsynaptic strength and unmasked LTD onto IT Type B neurons, without effect on ET Type A cells. These findings highlight motivation to stratify pyramidal cells in studies examining how ethanol and other experiences alter PFC function. Moreover, these results suggest that binge drinking preferentially alters IT circuit function, providing further rationale for evaluating mGlu$_2$ and mGlu$_3$ receptor positive allosteric modulators as potential treatments for AUD.

In the current studies, we found that IA ethanol did not affect the hyperpolarization sag ratio of deep layer PFC pyramidal cells. While it is possible that opposing adaptations to multiple pyramidal cell subtypes might have obfuscated each other without perturbing the overall sag ratio frequency distribution, the most parsimonious explanation for the present findings is that the sag ratio is generally static in adult PFC pyramidal cells and is not affected by IA ethanol. In support of that conclusion, and in accordance with many other studies (Anastasiades et al., 2018a; Anastasiades et al., 2018b; Gee et al., 2012; Lee et al., 2014; Seong and Carter, 2012), R$_m$ and other physiological parameters also clearly distinguished Type A and Type B neurons after IA ethanol treatment. The retained set of differences across several parameters is consistent with a veritable dissociation between ET and IT pyramidal cells that is not altered by voluntary drinking. By contrast, previous studies by Salling et al. (Salling et al., 2018) found that exposure to IA ethanol during adolescence decreased hyperpolarization sag and HCN channel function in same cells. Two methodological considerations – the concentration of ethanol and subject sex – might have contributed to this discrepancy, but we believe the key determinant underlying the distinct findings is the developmental timing of ethanol consumption. The PFC undergoes tremendous adaptations and maturation during adolescence (Spear and Swartzwelder, 2014). Insults during adolescence, like binge drinking, may stunt these processes and generate immature phenotypes that persist into adulthood. Consistent with that notion, Salling et al. (Salling et al., 2018) observed that the sag ratio generally increases across adolescence, undergoing a rapid developmental increase between P28-P42. In that same study, adolescent IA ethanol (beginning P30) altered the sag ratio frequency distribution in adult animals such that Type A ET neurons did not develop increased HCN channel activity. In the present study, however, animals first received IA ethanol during young adulthood (beginning P42-P49), after which the hyperpolarization sag has matured. In parallel to the developmental

differences in HCN channel function, extrasynaptic, tonic $GABA_A$ receptor currents are not observed in the frontal cortex of young animals (Centanni et al., 2017; Salling and Harrison, 2014), but these currents develop over time following increased expression or α5 and/or δ subunits (Centanni et al., 2017; Lee and Maguire, 2014). Adolescent CIE prevents the development of these $GABA_A$ receptor tonic currents, halting the PFC in an adolescent-like state (Centanni et al., 2017). The current studies, in concert with those by Salling et al. (Salling et al., 2018), paint a similar picture for PFC HCN channels, whereby adolescence represents a critical window that renders the PFC sensitive to certain deleterious effects of ethanol (Spear and Swartzwelder, 2014).

The present findings build upon the existing literature examining how voluntary drinking alters fast neurotransmission in the rodent PFC. This literature includes mixed results, as previous studies found that voluntary drinking increased (Klenowski et al., 2016), decreased (Crowley et al., 2019), or did not alter (Cannady et al., 2020) excitatory drive onto pyramidal cells in the prelimbic or anterior cingulate areas. Several technical differences between studies may contribute to this variation. Above all else, Crowley et al. (Crowley et al., 2019) performed recordings in layers 2/3, while all other studies described adaptations within layer 5. As the present findings indicate that voluntary ethanol differentially affects subtypes of PFC pyramidal cells, we fully expect distinct adaptations across the anatomically and molecularly varied cortical layers. Here, in layer 5, we observed increased synaptic strength in a subset of pyramidal cells, consistent with the modest effect observed by Klenowski et al. (Klenowski et al., 2016). We also believe these findings are not inconsistent with the negative results obtained by Cannady et al. (Cannady et al., 2020), considering the effect size, cell type-specificity, and additional methodological considerations. For one, to our knowledge, the present study is the first to examine ethanol's effects on PFC excitatory transmission using a potassium-based internal solution. Despite their utility in controlling membrane voltage and in sampling distal synapses, cesium-based internal solutions used in previous studies preclude detecting synaptic adaptations mediated by altered potassium channel function. In addition, the previous layer 5 studies relied exclusively on male subjects; in the current experiments, we included all mice. While these studies were not powered to detect modest sex differences, it is possible that a stronger effect size on female mice may have generated a larger composite effect. Another key methodological difference between the current studies and previous work is the timing of animal sacrifice for recordings. While all studies under discussion were conducted one day after the previous drinking session, mice in the present experiments were sacrificed during the first half of the light phase while rodents in previous studies were sacrificed during the dark phase. The formation and maintenance of neocortical synapses varies across the circadian rhythm (Liston et al., 2013) and behaviors relevant to alcohol-and drug-seeking exhibit diurnal variation (Parekh and McClung, 2015), thus the time of animal sacrifice is an important divergence between this work and previous studies. Along that line, the single time points for ethanol exposure and for *ex vivo* electrophysiology each represent a clear limitation to the current studies. Future research incorporating longitudinal experimental designs is likely to help reconcile differences between this and previous studies and to identify persistent adaptations relevant for abstinent individuals. With that in mind, future studies would also

benefit from probing the relationship between synaptic physiology and AUD-relevant behaviors following IA ethanol exposure.

ET and IT pyramidal cells differ in several morphological and physiological parameters (Anastasiades et al., 2018b; Clarkson et al., 2017; Dembrow et al., 2010; Gee et al., 2012; Lee et al., 2014; Morishima et al., 2011; Seong and Carter, 2012). Distinct but related schemes have been developed to functionally separate these neurons, most of which involve the hyperpolarization sag in some way. Here, we confirmed that pyramidal cells that project to five different target regions can be readily classified as ET or IT by sag ratio alone. Accurate classifications were obtained for most neurons sampled using *a priori* virus-assisted labeling (89% total: 19/23 ET cells and 30/32 IT cells). This scheme represents a generalizable means to add cell type-specific experimental design to future studies examining PFC function where genetic or anatomical approaches are not tractable. Such a design has the potential to uncover modest or otherwise undetectable adaptations, as evidenced by the present finding that only Type B neurons displayed synaptic adaptations following IA ethanol. Nonetheless, Type B neurons still represent a broad and heterogeneous conglomeration of pyramidal cells (Lee et al., 2020; Tasic et al., 2016; Tasic et al., 2018). Besides many transcriptomic differences, the current studies revealed that pyramidal cells projecting to the NAC, DMS, and BLA, all exhibited properties of Type B neurons, begging the question: which of these output circuits, if any, were altered by IA ethanol? We fully expect that future experiments using circuit mapping techniques will reveal more specific adaptations to PFC pyramidal cell subtypes following binge drinking and in models of dependence. Several other types of IT neurons not surveyed here, including those that project to claustrum, bed nucleus of the stria terminalis, and other neocortical targets, should also be evaluated in future studies.

PFC molecular taxonomy suggests IT cells may be comprised of up to 40 distinct subgroups (Tasic et al., 2016; Tasic et al., 2018). Future research may be able to leverage this heterogeneity to uncover the molecular determinants that guide ethanol-induced adaptations to PFC function. The differential expression of many protein types contributes to the varied transcriptomes of pyramidal cells, but G protein-coupled receptors (GPCRs) represent exciting candidate molecules that may modify synaptic strength and plasticity following ethanol exposure. For example, several studies have demonstrated that the dopamine D1 and D2 receptors guide distinct effects on ET versus IT pyramidal cells (Anastasiades et al., 2018a; Clarkson et al., 2017; Gee et al., 2012; Leyrer-Jackson and Thomas, 2019; Seong and Carter, 2012). Perhaps oscillations in PFC dopamine during ethanol experiences facilitate varied synaptic adaptations based on cell type-specific expression of dopamine receptors. Indeed, biased disruptions to dopamine receptor function have been observed following CIE exposure (Trantham-Davidson et al., 2014), suggesting dopamine signaling is also likely to guide specific adaptations following voluntary ethanol exposure. Similarly, serotonin and acetylcholine act on GPCRs to differentially regulate PFC pyramidal cells based on intrinsic physiology and projection target (Avesar and Gulledge, 2012; Baker et al., 2018; Elliott et al., 2018), and these systems may be involved in how ethanol experiences shape PFC function. Unlike the previously discussed neuromodulatory GPCRs, $mGlu_3$ and $mGlu_5$ receptors are expressed in the vast majority of pyramidal cell subtypes, including both IT and ET cells (Lee et al., 2020; Tasic et al., 2018). At face value, it may seem less likely that

mGlu receptor signaling contributed to the IT-specific synaptic adaptations observed in the present studies. Nonetheless, several forms of signaling dependent on $mGlu_5$ receptors are disrupted following ethanol exposure (Joffe et al., 2018; Kasten et al., 2019), raising the possibility that increased postsynaptic strength in IT neurons may have followed from disrupted mGlu receptor LTD. Relatively mild stress disrupts PFC LTD through specific changes to discrete signaling pathways downstream from $mGlu_5$ receptors and Homer proteins (Joffe et al., 2017; Joffe et al., 2019), and IA ethanol exposure may disrupt LTD through similar mechanisms as observed in many other brain regions (Quadir et al., 2016; Szumlinski et al., 2005). Collectively, neuromodulatory receptors and other GPCRs merit further investigation as means to remediate PFC dysfunction following binge drinking and dependence.

Type B neurons displayed enhanced postsynaptic strength and presynaptic plasticity following IA ethanol; are these two distinct phenomena or could they be explained by one common adaptation? We believe the latter, as enhanced postsynaptic strength at MDT synapses onto pyramidal cells could manifest as increased presynaptic LTD independent of changes to $mGlu_2$ function *per se*. In ethanol-naïve subjects, PFC $mGlu_2$-LTD is small but non-negligible following electrical stimulation. Even when pathways required for postsynaptic $mGlu_3$-LTD are blocked, we have found that LY379268 application still decreases electrically-evoked EPSCs by about 10% (Joffe et al., 2017; Joffe et al., 2019). This decrease is likely mediated by synapses arising from the MDT, which, when isolated with optogenetics, are attenuated by nearly 40% following selective $mGlu_2$ receptor activation (Joffe et al., 2020a). Therefore, if the IA ethanol-induced increase in postsynaptic strength occurred at synapses receiving glutamate from the MDT, the relative magnitude of $mGlu_2$-LTD could be enhanced in the absence of direct adaptations to any presynaptic molecules. Consistent with this interpretation, while neither the basal PPR nor sEPSC frequency were affected, IA ethanol treatment unmasked a long-term increase in PPR following LY379268 application, consistent with presynaptic $mGlu_2$-LTD at MDT terminals (Joffe et al., 2020a; Johnson et al., 2017). Nonetheless, future experiments will need to directly test the hypothesis that MDT-PFC transmission is selectively altered by IA ethanol. Leveraging optogenetic tools to isolate inputs from the MDT and other sources of PFC glutamate may shed light on the specific neurocircuits altered by binge drinking and in models of ethanol dependence.

5. Conclusion

PFC pyramidal cell heterogeneity arises from cell type-specific differences in anatomy, physiology, and molecular programming. This rich source of variation provides opportunities for developing new treatments tailored to circuit-specific differences observed in a preclinical disease model. The current findings improve our understanding of how drinking affects PFC function and underscore motivation for continued translational studies examining mGlu receptor modulators as potential AUD treatments.

Supplementary Material

Refer to Web version on PubMed Central for supplementary material.

Acknowledgements

References

Abernathy K, Chandler LJ, Woodward JJ, 2010. Alcohol and the prefrontal cortex. Int Rev Neurobiol 91, 289–320. [PubMed: 20813246]

Anastasiades PG, Boada C, Carter AG, 2018a. Cell-Type-Specific D1 Dopamine Receptor Modulation of Projection Neurons and Interneurons in the Prefrontal Cortex. Cereb Cortex.

Anastasiades PG, Marlin JJ, Carter AG, 2018b. Cell-Type Specificity of Callosally Evoked Excitation and Feedforward Inhibition in the Prefrontal Cortex. Cell Rep 22, 679–692. [PubMed: 29346766]

Avesar D, Gulledge AT, 2012. Selective serotonergic excitation of callosal projection neurons. Front Neural Circuits 6, 12. [PubMed: 22454619]

Baker AL, O'Toole RJ, Gulledge AT, 2018. Preferential cholinergic excitation of corticopontine neurons. J Physiol 596, 1659–1679. [PubMed: 29330867]

Belknap JK, Crabbe JC, Young ER, 1993. Voluntary consumption of ethanol in 15 inbred mouse strains. Psychopharmacology (Berl) 112, 503–510. [PubMed: 7871064]

Blaine SK, Wemm S, Fogelman N, Lacadie C, Seo D, Scheinost D, Sinha R, 2020. Association of Prefrontal-Striatal Functional Pathology With Alcohol Abstinence Days at Treatment Initiation and Heavy Drinking After Treatment Initiation. Am J Psychiatry 177, 1048–1059. [PubMed: 32854534]

Bohnsack JP, Hughes BA, O'Buckley TK, Edokpolor K, Besheer J, Morrow AL, 2018. Histone deacetylases mediate GABAA receptor expression, physiology, and behavioral maladaptations in rat models of alcohol dependence. Neuropsychopharmacology 43, 1518–1529. [PubMed: 29520058]

Boyce-Rustay JM, Janos AL, Holmes A, 2008. Effects of chronic swim stress on EtOH-related behaviors in C57BL/6J, DBA/2J and BALB/cByJ mice. Behav Brain Res 186, 133–137. [PubMed: 17822784]

Cannady R, Nimitvilai-Roberts S, Jennings SD, Woodward JJ, Mulholland PJ, 2020. Distinct Region- and Time-Dependent Functional Cortical Adaptations in C57BL/6J Mice after Short and Prolonged Alcohol Drinking. eNeuro 7.

Carlen M, 2017. What constitutes the prefrontal cortex? Science 358, 478–482. [PubMed: 29074767]

Centanni SW, Burnett EJ, Trantham-Davidson H, Chandler LJ, 2017. Loss of delta-GABAA receptor-mediated tonic currents in the adult prelimbic cortex following adolescent alcohol exposure. Addict Biol 22, 616–628. [PubMed: 26804056]

Clarkson RL, Liptak AT, Gee SM, Sohal VS, Bender KJ, 2017. D3 Receptors Regulate Excitability in a Unique Class of Prefrontal Pyramidal Cells. J Neurosci 37, 5846–5860. [PubMed: 28522735]

Collins DP, Anastasiades PG, Marlin JJ, Carter AG, 2018. Reciprocal Circuits Linking the Prefrontal Cortex with Dorsal and Ventral Thalamic Nuclei. Neuron 98, 366–379 e364. [PubMed: 29628187]

Crowley NA, Magee SN, Feng M, Jefferson SJ, Morris CJ, Dao NC, Brockway DF, Luscher B, 2019. Ketamine normalizes binge drinking-induced defects in glutamatergic synaptic transmission and ethanol drinking behavior in female but not male mice. Neuropharmacology 149, 35–44. [PubMed: 30731135]

Dembrow NC, Chitwood RA, Johnston D, 2010. Projection-specific neuromodulation of medial prefrontal cortex neurons. J Neurosci 30, 16922–16937. [PubMed: 21159963]

Di Menna L, Joffe ME, Iacovelli L, Orlando R, Lindsley CW, Mairesse J, Gressens P, Cannella M, Caraci F, Copani A, Bruno V, Battaglia G, Conn PJ, Nicoletti F, 2018. Functional partnership between mGlu3 and mGlu5 metabotropic glutamate receptors in the central nervous system. Neuropharmacology 128, 301–313. [PubMed: 29079293]

Elliott MC, Tanaka PM, Schwark RW, Andrade R, 2018. Serotonin Differentially Regulates L5 Pyramidal Cell Classes of the Medial Prefrontal Cortex in Rats and Mice. eNeuro 5.

Gabbott PL, Warner TA, Jays PR, Salway P, Busby SJ, 2005. Prefrontal cortex in the rat: projections to subcortical autonomic, motor, and limbic centers. J Comp Neurol 492, 145–177. [PubMed: 16196030]

Gee S, Ellwood I, Patel T, Luongo F, Deisseroth K, Sohal VS, 2012. Synaptic activity unmasks dopamine D2 receptor modulation of a specific class of layer V pyramidal neurons in prefrontal cortex. J Neurosci 32, 4959–4971. [PubMed: 22492051]

Haun HL, Griffin WC, Lopez MF, Solomon MG, Mulholland PJ, Woodward JJ, McGinty JF, Ron D, Becker HC, 2018. Increasing Brain-Derived Neurotrophic Factor (BDNF) in medial prefrontal cortex selectively reduces excessive drinking in ethanol dependent mice. Neuropharmacology 140, 35–42. [PubMed: 30056122]

Hughes BA, Bohnsack JP, O'Buckley TK, Herman MA, Morrow AL, 2019. Chronic Ethanol Exposure and Withdrawal Impair Synaptic GABAA Receptor-Mediated Neurotransmission in Deep-Layer Prefrontal Cortex. Alcohol Clin Exp Res 43, 822–832. [PubMed: 30860602]

Hwa LS, Chu A, Levinson SA, Kayyali TM, DeBold JF, Miczek KA, 2011. Persistent escalation of alcohol drinking in C57BL/6J mice with intermittent access to 20% ethanol. Alcohol Clin Exp Res 35, 1938–1947. [PubMed: 21631540]

Joffe ME, Centanni SW, Jaramillo AA, Winder DG, Conn PJ, 2018. Metabotropic Glutamate Receptors in Alcohol Use Disorder: Physiology, Plasticity, and Promising Pharmacotherapies. ACS Chem Neurosci.

Joffe ME, Santiago CI, Engers JL, Lindsley CW, Conn PJ, 2017. Metabotropic glutamate receptor subtype 3 gates acute stress-induced dysregulation of amygdalo-cortical function. Mol Psychiatry.

Joffe ME, Santiago CI, Oliver KH, Maksymetz J, Harris NA, Engers JL, Lindsley CW, Winder DG, Conn PJ, 2020a. mGlu2 and mGlu3 Negative Allosteric Modulators Divergently Enhance Thalamocortical Transmission and Exert Rapid Antidepressant-like Effects. Neuron 105, 46–59 e43. [PubMed: 31735403]

Joffe ME, Santiago CI, Stansley BJ, Maksymetz J, Gogliotti RG, Engers JL, Nicoletti F, Lindsley CW, Conn PJ, 2019. Mechanisms underlying prelimbic prefrontal cortex mGlu3/mGlu5-dependent plasticity and reversal learning deficits following acute stress. Neuropharmacology 144, 19–28. [PubMed: 30326237]

Joffe ME, Winder DG, Conn PJ, 2020b. Contrasting sex-dependent adaptations to synaptic physiology and membrane properties of prefrontal cortex interneuron subtypes in a mouse model of binge drinking. Neuropharmacology, 108126.

Johnson KA, Mateo Y, Lovinger DM, 2017. Metabotropic glutamate receptor 2 inhibits thalamically-driven glutamate and dopamine release in the dorsal striatum. Neuropharmacology 117, 114–123. [PubMed: 28159646]

Kasten CR, Holmgren EB, Wills TA, 2019. Metabotropic Glutamate Receptor Subtype 5 in Alcohol-Induced Negative Affect. Brain Sci 9.

Klenowski PM, Fogarty MJ, Shariff M, Belmer A, Bellingham MC, Bartlett SE, 2016. Increased Synaptic Excitation and Abnormal Dendritic Structure of Prefrontal Cortex Layer V Pyramidal Neurons following Prolonged Binge-Like Consumption of Ethanol. eNeuro 3.

Koob GF, Volkow ND, 2016. Neurobiology of addiction: a neurocircuitry analysis. Lancet Psychiatry 3, 760–773. [PubMed: 27475769]

Kroener S, Mulholland PJ, New NN, Gass JT, Becker HC, Chandler LJ, 2012. Chronic alcohol exposure alters behavioral and synaptic plasticity of the rodent prefrontal cortex. PLoS One 7, e37541. [PubMed: 22666364]

Lee AT, Gee SM, Vogt D, Patel T, Rubenstein JL, Sohal VS, 2014. Pyramidal neurons in prefrontal cortex receive subtype-specific forms of excitation and inhibition. Neuron 81, 61–68. [PubMed: 24361076]

Lee J, Munguba H, Gutzeit VA, Singh DR, Kristt M, Dittman JS, Levitz J, 2020. Defining the Homo- and Heterodimerization Propensities of Metabotropic Glutamate Receptors. Cell Rep 31, 107605. [PubMed: 32375054]

Lee V, Maguire J, 2014. The impact of tonic GABAA receptor-mediated inhibition on neuronal excitability varies across brain region and cell type. Front Neural Circuits 8, 3. [PubMed: 24550784]

Leyrer-Jackson JM, Thomas MP, 2019. Dopaminergic D1 receptor effects on commissural inputs targeting layer V pyramidal subtypes of the mouse medial prefrontal cortex. Physiol Rep 7, e14256. [PubMed: 31650716]

Liston C, Cichon JM, Jeanneteau F, Jia Z, Chao MV, Gan WB, 2013. Circadian glucocorticoid oscillations promote learning-dependent synapse formation and maintenance. Nat Neurosci 16, 698–705. [PubMed: 23624512]

Morishima M, Morita K, Kubota Y, Kawaguchi Y, 2011. Highly differentiated projection-specific cortical subnetworks. J Neurosci 31, 10380–10391. [PubMed: 21753015]

Parekh PK, McClung CA, 2015. Circadian Mechanisms Underlying Reward-Related Neurophysiology and Synaptic Plasticity. Front Psychiatry 6, 187. [PubMed: 26793129]

Pava MJ, Woodward JJ, 2014. Chronic ethanol alters network activity and endocannabinoid signaling in the prefrontal cortex. Front Integr Neurosci 8, 58. [PubMed: 25100953]

Pleil KE, Lowery-Gionta EG, Crowley NA, Li C, Marcinkiewcz CA, Rose JH, McCall NM, Maldonado-Devincci AM, Morrow AL, Jones SR, Kash TL, 2015. Effects of chronic ethanol exposure on neuronal function in the prefrontal cortex and extended amygdala. Neuropharmacology 99, 735–749. [PubMed: 26188147]

Quadir SG, Santos JR, Campbell RR, Wroten MG, Singh N, Holloway JJ, Bal SK, Camarini R, Szumlinski KK, 2016. Homer2 regulates alcohol and stress cross-sensitization. Addict Biol 21, 613–633. [PubMed: 25916683]

Radke AK, Jury NJ, Kocharian A, Marcinkiewcz CA, Lowery-Gionta EG, Pleil KE, McElligott ZA, McKlveen JM, Kash TL, Holmes A, 2017. Chronic EtOH effects on putative measures of compulsive behavior in mice. Addict Biol 22, 423–434. [PubMed: 26687341]

Rodgers DA, Mc CG, 1962. Mouse strain differences in preference for various concentrations of alcohol. Q J Stud Alcohol 23, 26–33. [PubMed: 14493106]

Salling MC, Harrison NL, 2014. Strychnine-sensitive glycine receptors on pyramidal neurons in layers II/III of the mouse prefrontal cortex are tonically activated. J Neurophysiol 112, 1169–1178. [PubMed: 24872538]

Salling MC, Jane Skelly M, Avegno E, Regan S, Zeric T, Nichols E, Harrison NL, 2018. Alcohol consumption during adolescence in a mouse model of binge drinking alters the intrinsic excitability and function of the prefrontal cortex through a reduction in the hyperpolarization-activated cation current. J Neurosci.

Seif T, Chang SJ, Simms JA, Gibb SL, Dadgar J, Chen BT, Harvey BK, Ron D, Messing RO, Bonci A, Hopf FW, 2013. Cortical activation of accumbens hyperpolarization-active NMDARs mediates aversion-resistant alcohol intake. Nat Neurosci 16, 1094–1100. [PubMed: 23817545]

Seong HJ, Carter AG, 2012. D1 receptor modulation of action potential firing in a subpopulation of layer 5 pyramidal neurons in the prefrontal cortex. J Neurosci 32, 10516–10521. [PubMed: 22855801]

Shah MM, 2014. Cortical HCN channels: function, trafficking and plasticity. J Physiol 592, 2711–2719. [PubMed: 24756635]

Siciliano CA, Noamany H, Chang CJ, Brown AR, Chen X, Leible D, Lee JJ, Wang J, Vernon AN, Vander Weele CM, Kimchi EY, Heiman M, Tye KM, 2019. A cortical-brainstem circuit predicts and governs compulsive alcohol drinking. Science 366, 1008–1012. [PubMed: 31754002]

Spear LP, Swartzwelder HS, 2014. Adolescent alcohol exposure and persistence of adolescent-typical phenotypes into adulthood: a mini-review. Neurosci Biobehav Rev 45, 1–8. [PubMed: 24813805]

Szumlinski KK, Lominac KD, Oleson EB, Walker JK, Mason A, Dehoff MH, Klugmann M, Cagle S, Welt K, During M, Worley PF, Middaugh LD, Kalivas PW, 2005. Homer2 is necessary for EtOH-induced neuroplasticity. J Neurosci 25, 7054–7061. [PubMed: 16049182]

Tasic B, Menon V, Nguyen TN, Kim TK, Jarsky T, Yao Z, Levi B, Gray LT, Sorensen SA, Dolbeare T, Bertagnolli D, Goldy J, Shapovalova N, Parry S, Lee C, Smith K, Bernard A, Madisen L, Sunkin SM, Hawrylycz M, Koch C, Zeng H, 2016. Adult mouse cortical cell taxonomy revealed by single cell transcriptomics. Nat Neurosci 19, 335–346. [PubMed: 26727548]

Tasic B, Yao Z, Graybuck LT, Smith KA, Nguyen TN, Bertagnolli D, Goldy J, Garren E, Economo MN, Viswanathan S, Penn O, Bakken T, Menon V, Miller J, Fong O, Hirokawa KE, Lathia K, Rimorin C, Tieu M, Larsen R, Casper T, Barkan E, Kroll M, Parry S, Shapovalova NV, Hirschstein

D, Pendergraft J, Sullivan HA, Kim TK, Szafer A, Dee N, Groblewski P, Wickersham I, Cetin A, Harris JA, Levi BP, Sunkin SM, Madisen L, Daigle TL, Looger L, Bernard A, Phillips J, Lein E, Hawrylycz M, Svoboda K, Jones AR, Koch C, Zeng H, 2018. Shared and distinct transcriptomic cell types across neocortical areas. Nature 563, 72–78. [PubMed: 30382198]

Trantham-Davidson H, Burnett EJ, Gass JT, Lopez MF, Mulholland PJ, Centanni SW, Floresco SB, Chandler LJ, 2014. Chronic alcohol disrupts dopamine receptor activity and the cognitive function of the medial prefrontal cortex. J Neurosci 34, 3706–3718. [PubMed: 24599469]

Uylings HB, Groenewegen HJ, Kolb B, 2003. Do rats have a prefrontal cortex? Behav Brain Res 146, 3–17. [PubMed: 14643455]

Varodayan FP, Sidhu H, Kreifeldt M, Roberto M, Contet C, 2018. Morphological and functional evidence of increased excitatory signaling in the prelimbic cortex during ethanol withdrawal. Neuropharmacology 133, 470–480. [PubMed: 29471053]
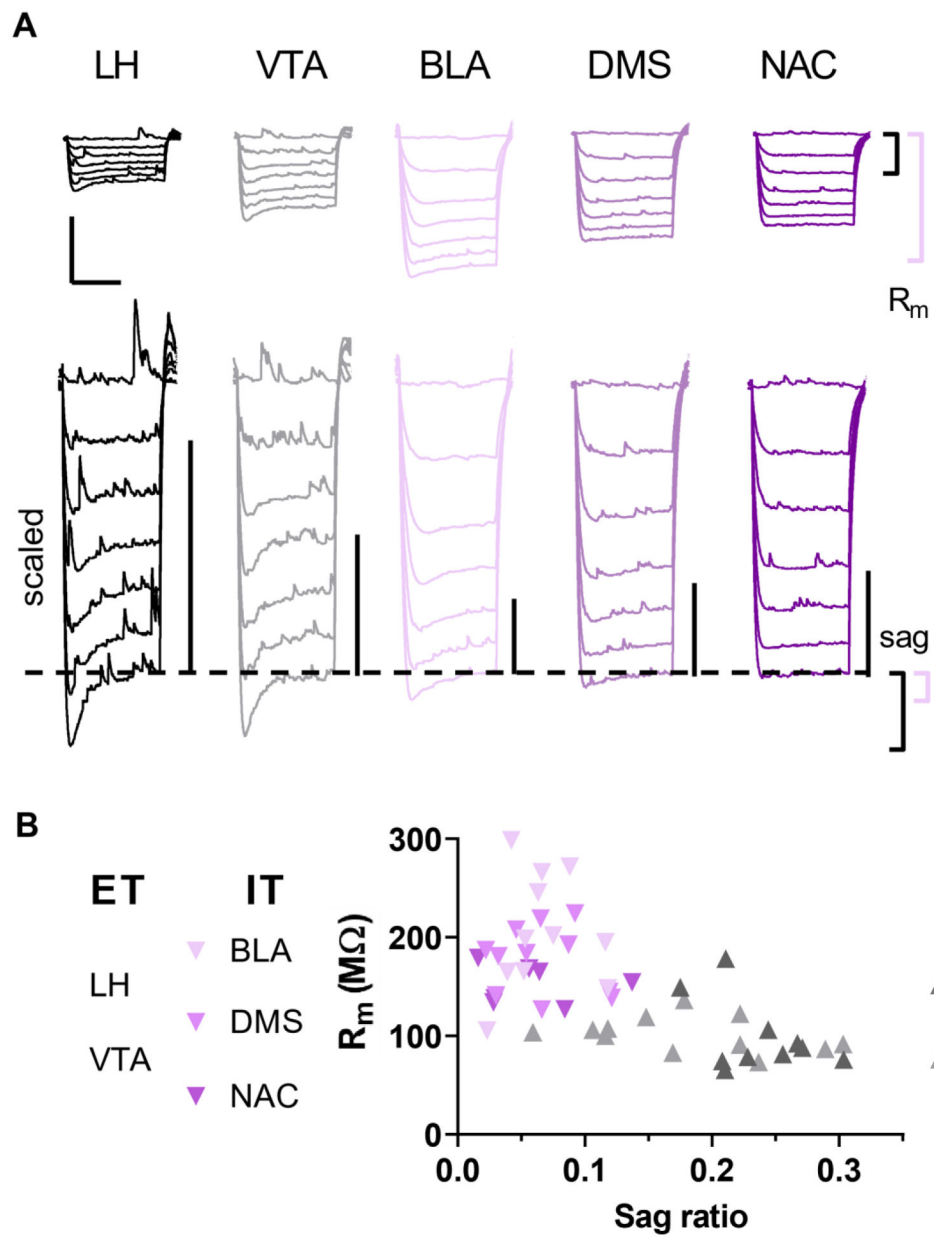
Figure 1.
Virus-assisted circuit mapping confirms **extra-telencephalic** (ET) and **intra-telencephalic** (IT) pyramidal cells respectively display Type A and Type B electrophysiological signatures
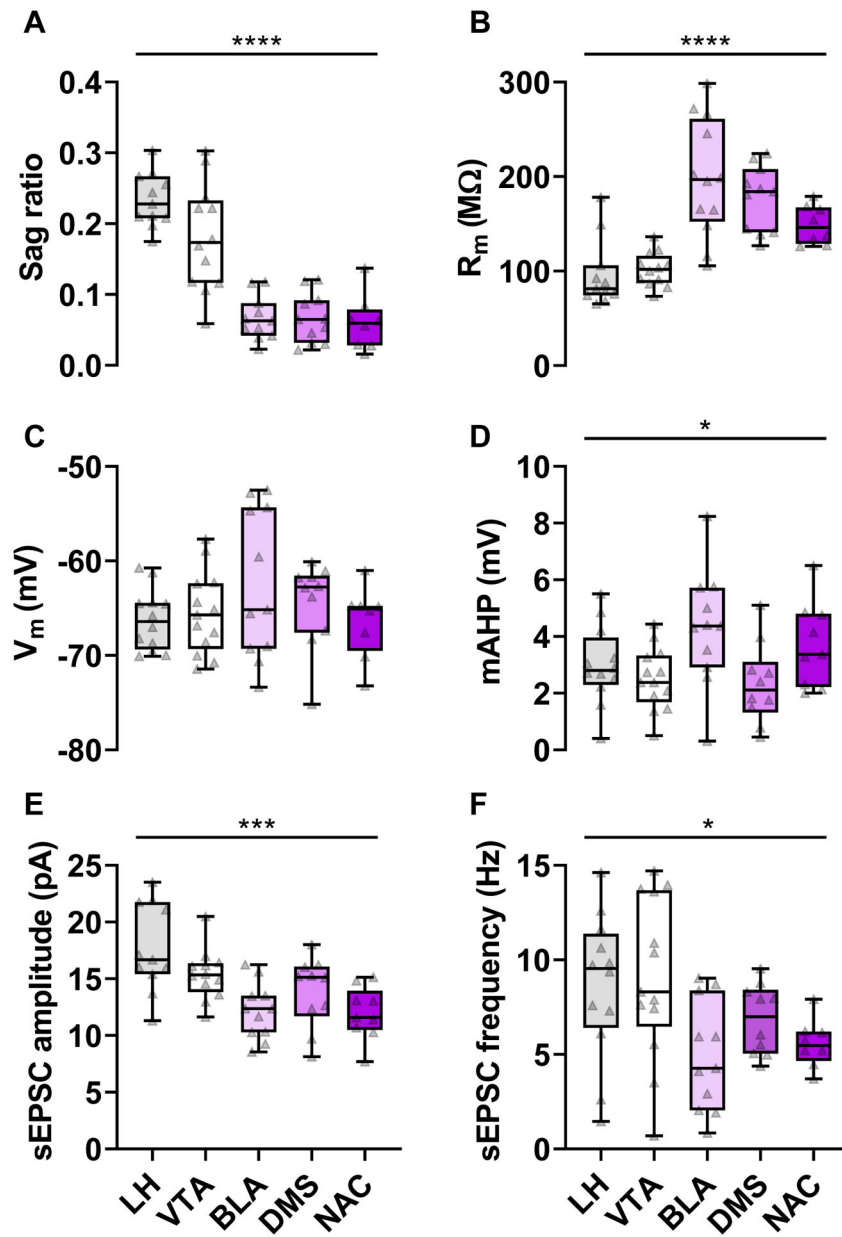
Figure 2.
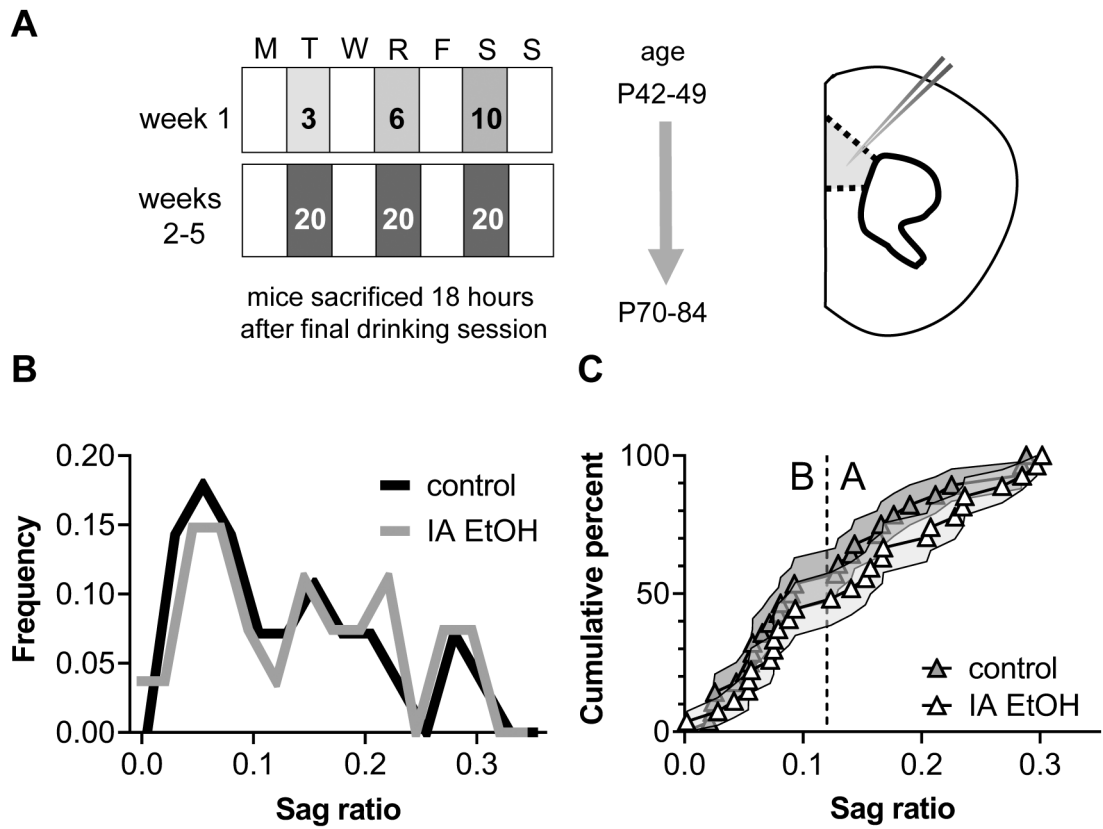Variation in membrane and synaptic physiology parameters related to pyramidal cell projection target

Figure 3.
Intermittent access (IA) ethanol in adulthood does not alter the hyperpolarization sag ratio of prefrontal cortex (PFC) pyramidal cells
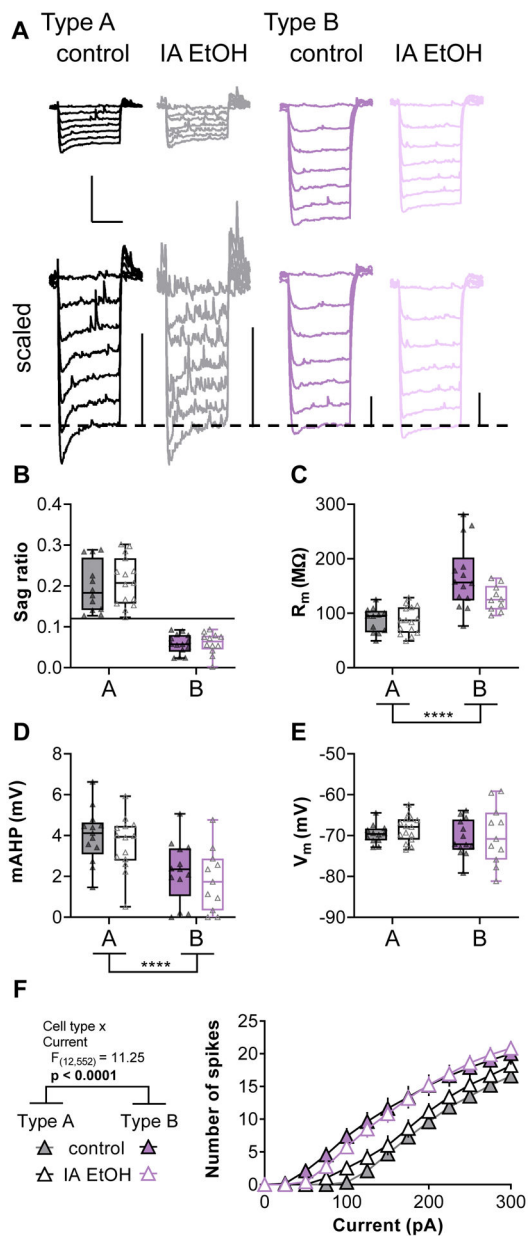
Figure 4.
Type A and Type B neurons display distinct membrane physiology properties, but none are affected by IA ethanol
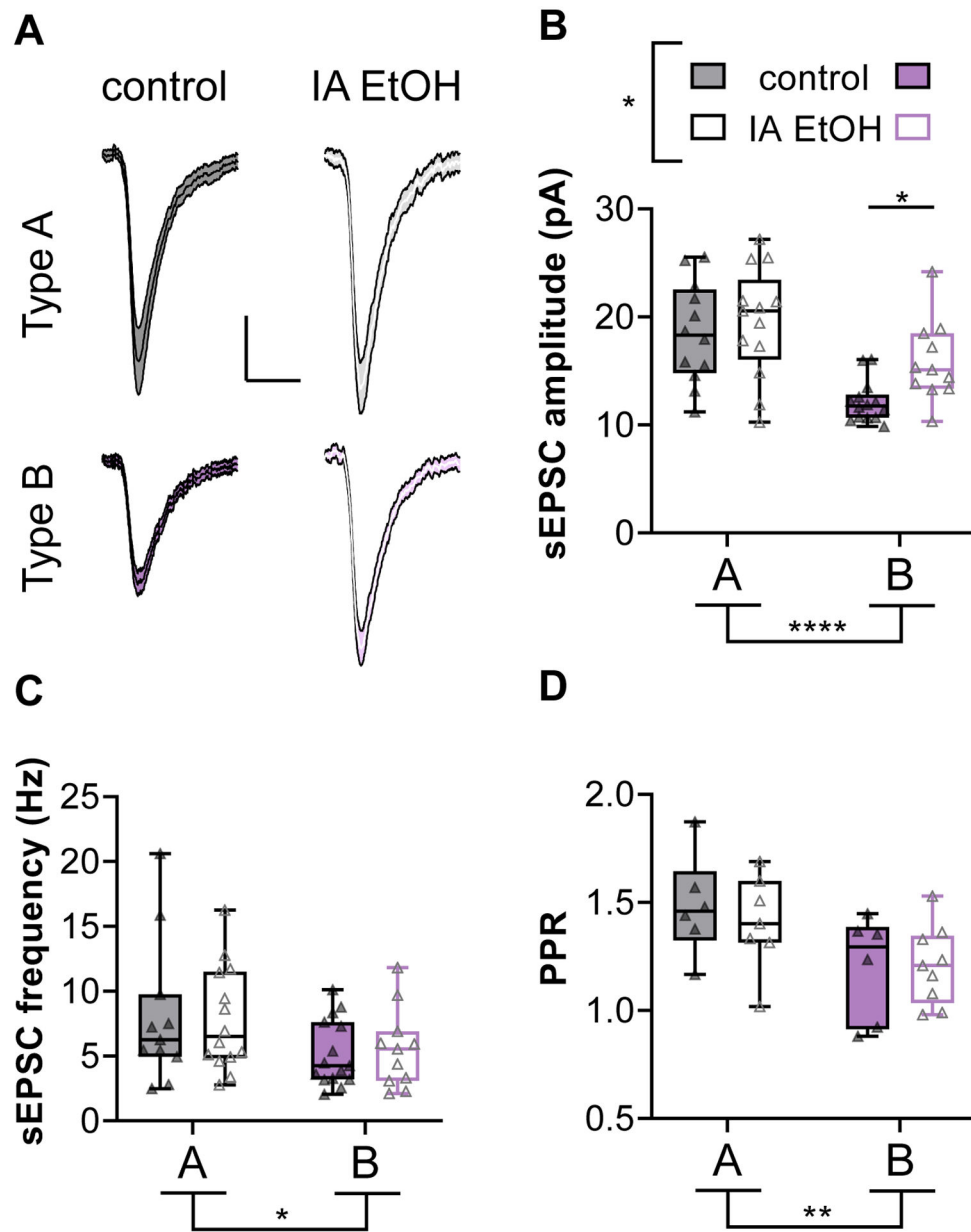
Figure 5.
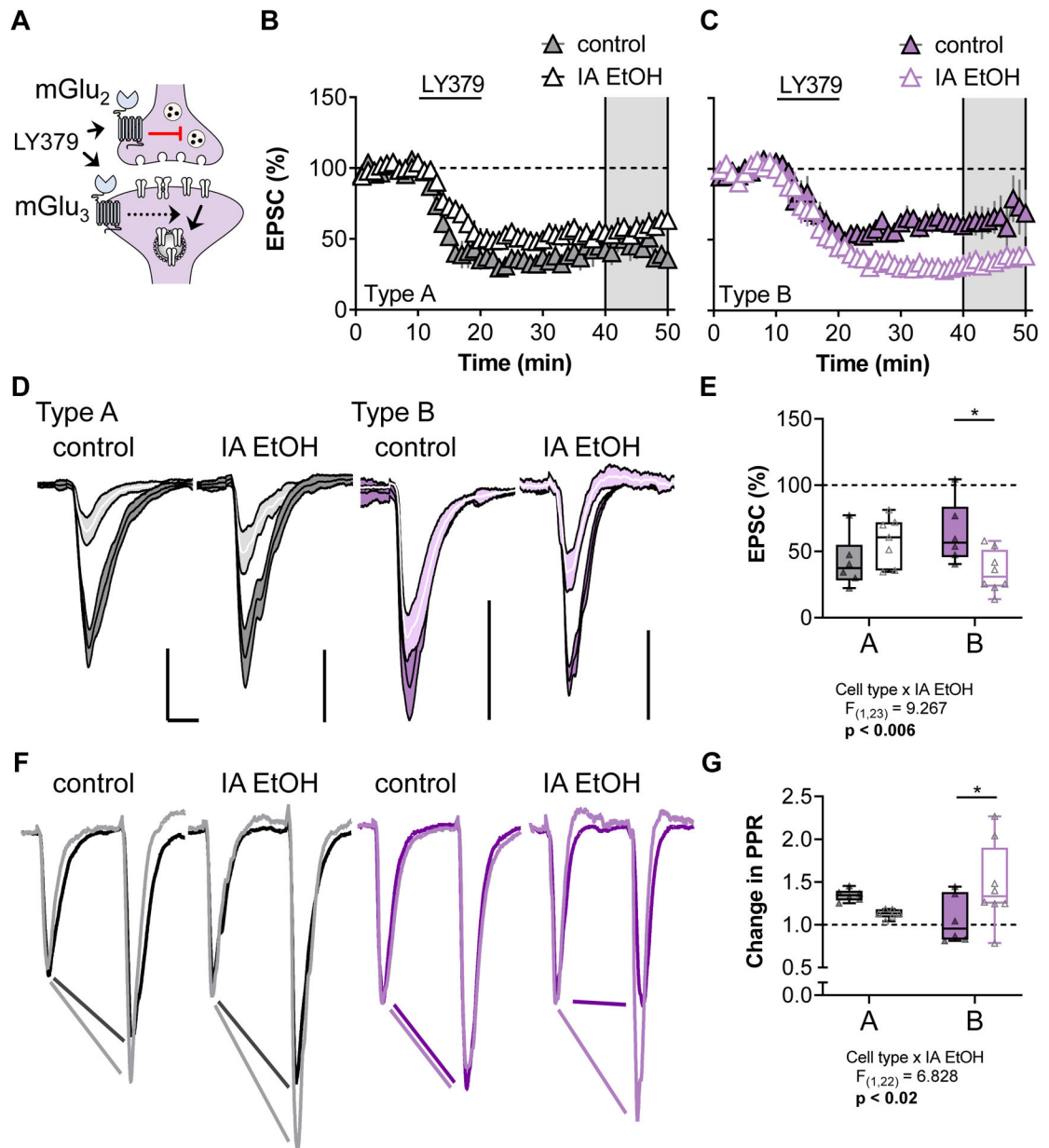IA ethanol selectively enhances postsynaptic strength onto Type B pyramidal cells

Figure 6.
IA ethanol enhances mGlu$_{2/3}$ long term depression (LTD) onto Type B pyramidal cells
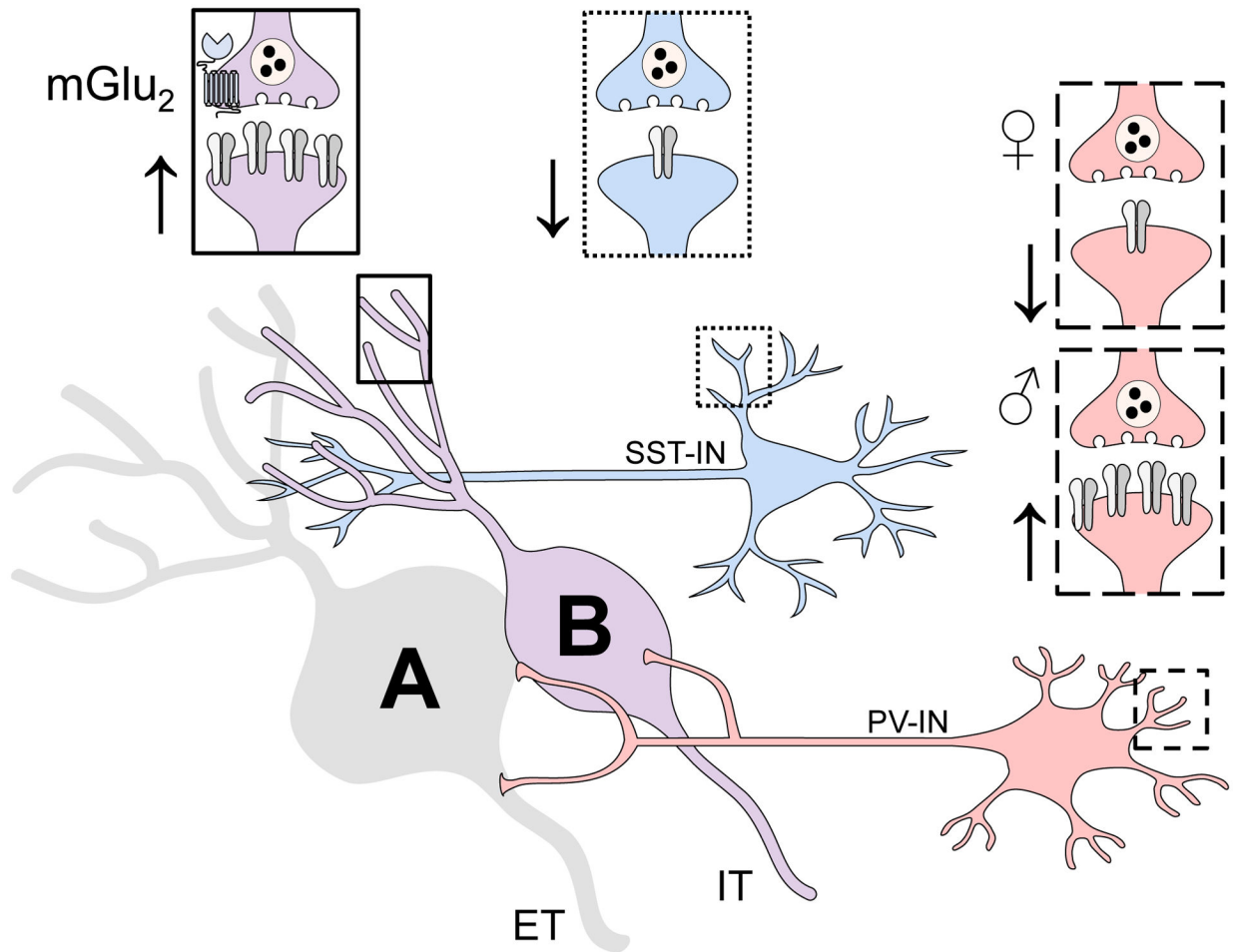
Figure 7.
Cell type-specific adaptations to glutamate transmission in the mouse prelimbic cortex
following intermittent access to ethanol